Paper

Enhancing the Speed of the 3D Finite Element Analysis by the Geometric Multigrid Method with Edge Elements

Vasil Spasov* Non-member
So Noguchi* Member
Hideo Yamashita* Member

This paper presents a fast electromagnetic field analysis by the 3D geometric multigrid method with edge elements. The multigrid method uses a symmetric Gauss-Seidel smoother with Conjugate Gradient acceleration. The convergence and computation speed of the V-cycle, W-cycle and full multigrid method using this smoother are compared with the conventional multigrid using Gauss-Seidel. Comparison is also made between the multigrid method and the ICCG method which is commonly used in the finite element analysis. The efficiency of the multigrid method is analyzed for meshes whose maximum aspect ratios vary in a wide range. It is proven that the multigrid method with the accelerated symmetric Gauss-Seidel outperforms the multigrid with Gauss-Seidel and the ICCG method. The multigrid method with the accelerated symmetric Gauss-Seidel shows stable convergence rate that does not deteriorate for bad quality meshes. It is robust against mesh distortion and parameter variations and is much faster than the conventional multigrid with Gauss-Seidel and the finite element method using ICCG.

Keywords: Geometric multigrid method, 3D finite element method, Edge elements, Magnetostatics

1. Introduction

In the last years the edge element geometric multigrid method (MGM) has proven to be very efficient for solving systems of equations resulting from the finite element analysis of electromagnetic fields [1]~[4]. In a well-designed MGM the number of arithmetic operations for the solution is proportional to the number of unknowns N [1]. For comparison, the widely used Incomplete Cholesky Conjugate Gradient (ICCG) method requires $N^{4/3}$ operations for 3D problems, which causes the solution time to increase strongly with the number of unknowns. This advantage, together with the better convergence rate, makes the MGM very attractive for the 3D analysis of electromagnetic fields.

In the MGM with nodal elements the smoothing is usually done by the Gauss-Seidel (GS) method. Unfortunately, when edge elements are used, the performance of MGM with the classical GS results in a poor convergence. In this case properly designed block GS smoothers are preferable [3] [4].

When the finite element mesh contains elements with large maximum aspect ratios, however, the edge MGM with the Gauss-Seidel smoother or its block variants converges slowly or even fails to converge [2] [5] [6]. This problem restricts the practical application of the conventional edge MGM to models with simple geometries whose meshes do not contain distorted elements.

To overcome this serious drawback, we propose an edge element MGM in which smoothing is done by the symmetric Gauss-Seidel accelerated by the Conjugate Gradient method. The convergence behavior and speed of the V-cycle, W-cycle and the full multigrid algorithms using this accelerated symmetric Gauss-Seidel (ASGS) smoother are analyzed for meshes whose maximum element aspect ratios vary in a wide range. In order to demonstrate the advantages of the proposed MGM with ASGS, comparison is made with the conventional MGM using Gauss-Seidel and with the finite element method using ICCG. Finally, the validity of MGM with ASGS is confirmed by comparing computed and measured electromagnetic force.

The results indicate that the proposed MGM with ASGS is considerably faster than the conventional solution strategies. It has stable convergence rate that does not depend significantly on the maximum element aspect ratio and material properties. The proposed MGM with ASGS is superior to MG with Gauss-Seidel and the finite element method using ICCG even for meshes with small number of unknowns and levels.

2. Finite Element Formulation

Ungauged magnetic vector potential formulation is used. The governing equation of the magnetostatic field is given by

$$\mathrm{rot}(\nu \mathrm{rot} \boldsymbol{A}) = \boldsymbol{J}, \quad \cdots\cdots\cdots\cdots\cdots\cdots\cdots\cdots (1)$$

where ν is the magnetic reluctivity, $\boldsymbol{A}$ is the magnetic vector potential and $\boldsymbol{J}$ is the current density.

The finite element discretization is based on first order hexahedral conforming edge elements [7]. The magnetic

* Graduate School of Engineering, Hiroshima University
1-4-1 Kagamiyama, Higashihiroshima 739-8527

vector potential is approximated by

$$\boldsymbol{A}(x,y,z) \approx \sum_{i=1}^{ne} a_i \boldsymbol{N}_i(x,y,z), \quad \cdots\cdots\cdots\cdots \quad (2)$$

where ne is the number of edges in the finite element mesh, a_i is the corresponding degree of freedom, namely the line integral of $\boldsymbol{A}$ along edge i and $\boldsymbol{N}_i$ is the edge shape function.

It has been shown that the convergence of the ICCG method is very sensitive to the continuity of the source current density [8]. In order to achieve a high convergence rate of the ICCG method, the continuity of the source current density in this paper is satisfied by using the method in reference (9).

3. The Geometric Multigrid Method

3.1 Types of Multigrid Algorithms The basic idea of the geometric multigrid method is to work with a sequence of meshes of different size. The high-frequency components of the error of the numerical solution are eliminated by iterative smoothing methods on the fine mesh. The low-frequency components of the error are interpolated to the coarse mesh. There they become high frequency errors, which are eliminated using the same iterative methods.

Due to the lack of gauge in the finite element formulation, the resulting coefficient matrix of equation (1) is singular. For this reason at the coarsest mesh the problem is solved by the ICCG method. Since the number of unknowns of this mesh is small, this solution is not time and memory consuming. This procedure, called *the coarse grid correction scheme*, is briefly described below [10]:

Step 1: Relax a few times on $S_2 \cdot x_2 = b_2$ to obtain an approximate solution $\tilde{x}_2$. Here S_2 is the matrix of the fine mesh, x_2 and b_2 are the vector of unknowns and the source vector, respectively. This step is called *smoothing*.

Step 2: Compute the residual vector $r_2 = b_2 - S_2 \cdot \tilde{x}_2$.

Step 3: Project the residual vector on the coarse mesh using the restriction operator $r_1 = R \cdot r_2$.

Step 4: Solve the residual equation $S_1 \cdot e_1 = r_1$ to obtain an approximation of the error e_1.

Step 5: Interpolate e_1 to the fine mesh using the prolongation operator $e_2 = P \cdot e_1$.

Step 6: Compute the improved solution $x_2 = \tilde{x}_2 + e_2$.

Step 7: Start a new iterative cycle by doing again smoothing.

The coarse grid correction scheme can be used recursively when solving the residual equation at *Step 4*. If the coarse grid correction scheme is performed recursively one time at each level, the widely used V-cycle multigrid is obtained. Another efficient algorithm is the W-cycle multigrid algorithm. The V-cycle and W-cycle multigrid algorithms are shown in Fig. 1.

As seen in Fig. 1, the V-cycle and the W-cycle multigrid algorithms obtained their names according to the shape of the cycle they perform. The smoothing in

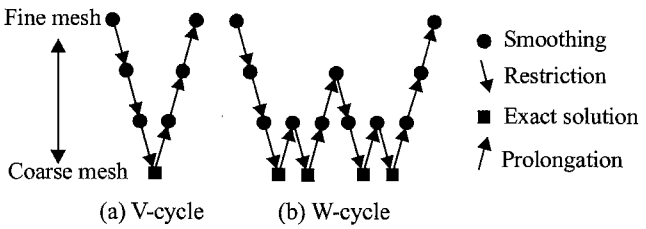

Fig. 1. V- and W-cycle multigrid algorithms with four levels.

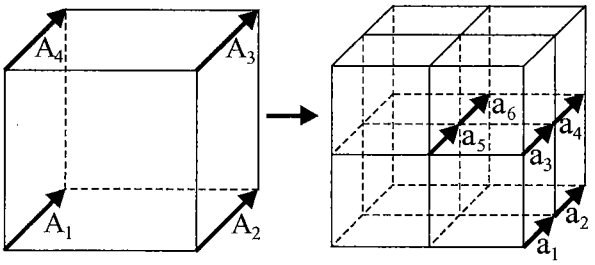

Fig. 2. Definition of the prolongation operator.

these algorithms can be carried out before reaching the coarsest mesh as well as after the coarse mesh computations. Therefore two separate names are used, namely pre-smoothing and post-smoothing. The existence of pre-smoothing and post-smoothing steps as well as the number of smoothing iterations per cycle can be freely defined by the user and open a wide area for investigation.

3.2 Choosing the Grid Transfer Operators The efficiency of the MGM strongly depends on the choice of the grid transfer operators. To interpolate the edge values from the coarse to the finer mesh, a prolongation operator has to be defined. Additionally, a restriction operator is needed for projection of the edge values from the fine to the coarser mesh.

To define the prolongation operator, the mesh refinement for the MGM will be discussed. Initially a very coarse mesh is generated designated as level $q-1$. Then every hexahedron is uniformly split into eight smaller hexahedra as shown in Fig. 2. In this way the mesh for the next level q of MGM is generated. This procedure is repeated until a mesh is obtained which accurately describes the magnetic field. By dissecting the hexahedron at level $q-1$ into eight hexahedra at level q, every face F^{q-1} is replaced by four new faces $F_1^q, \cdots, F_4^q$.

The prolongation operator must fulfill the requirement of flux conservation during the mesh refinement [3][4]. For this reason the magnetic flux across a face of an element from the coarse mesh must be equal to the sum of the fluxes across the four replacing faces of the fine mesh:

$$\int_{F^{q-1}} (\nabla \times \boldsymbol{A}) \cdot d\boldsymbol{F} = \sum_{k=1}^{4} \int_{F_k^q} (\nabla \times \boldsymbol{A}) \cdot d\boldsymbol{F} \quad \cdots \quad (3)$$

Based on (3), we constructed the following prolongation operator that fulfills the requirement of flux conservation [1][4]:

$$\begin{Bmatrix} a_1 \\ a_2 \\ a_3 \\ a_4 \\ a_5 \\ a_6 \end{Bmatrix} = \frac{1}{2} \begin{bmatrix} 0 & 1 & 0 & 0 \\ 0 & 1 & 0 & 0 \\ 0 & 1/2 & 1/2 & 0 \\ 0 & 1/2 & 1/2 & 0 \\ 1/4 & 1/4 & 1/4 & 1/4 \\ 1/4 & 1/4 & 1/4 & 1/4 \end{bmatrix} \begin{Bmatrix} A_1 \\ A_2 \\ A_3 \\ A_4 \end{Bmatrix} \quad (4)$$

A_i and a_i in (4) designate the edge values of the coarse and the fine mesh, respectively, as shown in Fig. 2.

The restriction operator R is chosen as the transpose of the prolongation operator P, i.e.

$$[R] = c\,[P]^T \quad \cdots\cdots (5)$$

The parameter c in (5) is a constant used to speed-up the performance of MGM [10]. The choice of c in the case of nodal elements was studied in reference (11). In the next chapter of this paper we shall analyze the choice of the parameter c for edge elements.

3.3 Algorithm of the ASGS Smoother The choice of the smoother is crucial for the performance of MGM. When nodal elements are used, smoothing is usually done by the Gauss-Seidel method. Unfortunately, for edge elements the MGM with the classical GS has a poor convergence. Therefore properly designed block GS smoothers are used.

When the finite element mesh contains distorted elements with large aspect ratios, however, the edge MGM with the Gauss-Seidel or its block variants converges slowly or even fails to converge. To overcome this serious drawback, we propose an edge element MGM in which smoothing is done by the symmetric Gauss-Seidel accelerated by the conjugate gradient method. The algorithm of this accelerated symmetric Gauss-Seidel smoother is [12]~[14]:

1. Given an initial guess x_0, compute:

$r_0 = b - Dx_0 - Ux_0$

2. Perform smoothing iterations ($i = 1, 2, 3, \cdots$):

$D\omega_i = r_{i-1} - L(x_{-1} + \omega_{i-1})$
$q_i = D\omega_i$
$\gamma_1 = q_i^T \omega_i$
if (i.eq.1) then
  $\beta = 0$
else
  $\beta = \gamma_1/\gamma_2$
endif
$v_i = q_i + \beta v_{i-1}$
$(D+U)z_i = q_i$
$p_i = z_i + \beta p_{i-1}$
$\alpha = \gamma_1/(p_i^T(2v_i - Dp_i))$
$\gamma_2 = \gamma_1$
$r_i = r_{i-1} - \alpha v_i$
$x_i = x_{i-1} - \alpha p_i$

L and U in this algorithm are the lower and upper triangle of the global matrix, and D is the diagonal. Here r is the residual vector, x is the vector with the unknown values of the magnetic vector potential and b is the right-hand side. The results in this paper are obtained with zero initial values of the magnetic vector potential, that is $x_0 = 0$.

The arrays ω, v and p are auxiliary arrays, whose starting values are zero. The superscript "T" is used for "transposed".

The variables β, γ_1 and γ_2 are parameters used during the acceleration.

The scalar α in the above algorithm is an acceleration parameter that speeds up the convergence of symmetric GS. As seen, α is determined fully automatically during the solution and its computation is not expensive. For this reason we preferred the Conjugate Gradient acceleration to the Chebishev acceleration. The Chebishev acceleration depends on parameters that are computationally expensive to determine for 3D problems, such as good estimates of the smallest and largest eigenvalues of iteration matrix [12].

Concerning the computational efficiency of ASGS, the work required by the Conjugate Gradient acceleration is small as compared to the work by the symmetric Gauss-Seidel. Therefore, one iteration by the accelerated symmetric Gauss-Seidel is not much more expensive than a simple symmetric GS iteration.

4. Analysis of the Efficiency of MGM with ASGS

In order to analyze the efficiency of the MGM with the newly proposed ASGS smoother, two examples of application will be discussed. The first example, shown in Fig. 3(a), is a current-fed coil with iron core, surrounded by a shield. The exciting current is 1 A and the relative permeability of iron is 1000. The finite element formulation is given by (1). Edge hexahedra are used. Due to the symmetry, only one eight of the coil is analyzed.

This simple model allows to change easily the maximum element aspect ratio while retaining the same number of elements and edges in the mesh. It has been shown that the convergence of MGM depends on the maximum element aspect ratio ($R_{\max}$) rather than the average mesh quality [2] [5] [6]. For this reason, we shall use $R_{\max}$ as reference and not the average mesh quality.

To investigate the effect of the maximum element

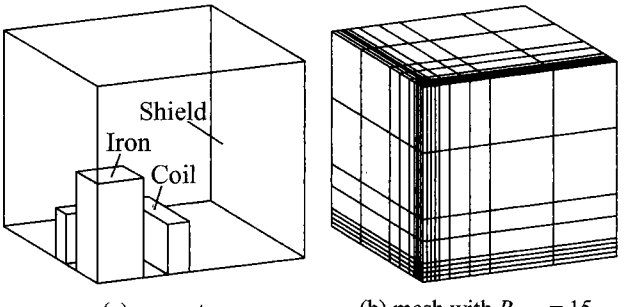

(a) geometry (b) mesh with $R_{max} = 15$

Fig. 3. Geometry and mesh of one eight of the coil.

Table 1. Discretization data for the coil.

Level	No. of unknowns	No. of elements
1	2420	648
2	17404	5184
3	131720	41472
4	1024336	331776

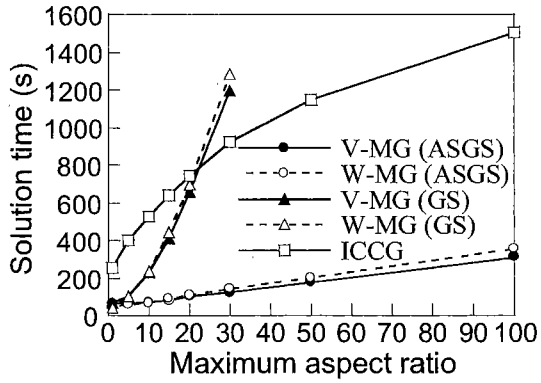

Fig. 4. Effect of maximum aspect ratio on the solution time.

aspect ratio on the convergence of MGM, meshes of aspect ratios from 1 to 100 are analyzed. The element aspect ratio is defined as the ratio of the length of the longest edge of the hexahedron to the length of its shortest edge. Thus the mesh with $R_{\max} = 1$ is composed of cubes while the mesh with $R_{\max} = 100$ contains highly distorted elements. Fig. 3(b) shows the mesh with $R_{\max} = 15$.

The numerical analysis is carried out by the V-cycle and W-cycle MGM with four nested meshes detailed in Table 1.

Fig. 4 compares the efficiency of MGM using ASGS, the conventional MGM with GS and the scaled ICCG method for meshes of different maximum aspect ratios. All computations in this paper are performed on a 2 GHz Pentium IV with 2 GByte RAM. The solution times in this figure and later are only the time to solve the systems of equations, these do not include the times for preprocessing, making the matrix and reading and writing the data files in MGM.

Fig. 4 shows that MGM using ASGS and MGM with GS result in similar solution times for meshes with $R_{\max} = 1$. Such cubic meshes, however, are usually not used in the practical MGM, since they lead to unacceptably large number of elements in the finest mesh. As seen, the efficiency of MGM with GS decreases rapidly with the increase of the maximum element aspect ratio. The advantages of MGM with GS over ICCG are lost for aspect ratios greater than 20. Moreover, MGM with GS does not converge to a residual of 10^{-6} for maximum aspect ratios above 30. In contrast, the increase of $R_{\max}$ does not significantly deteriorate the performance of MGM with ASGS. Fig. 4 indicates that V-cycle MGM with ASGS is the fastest for all aspect ratios.

The results in the paper are with equal number of pre- and post-smoothing iterations n_{si}. When cubic mesh is used, MGM with ASGS is the fastest with $n_{si} = 2$, while MGM with GS is the fastest with $n_{si} = 1$. With

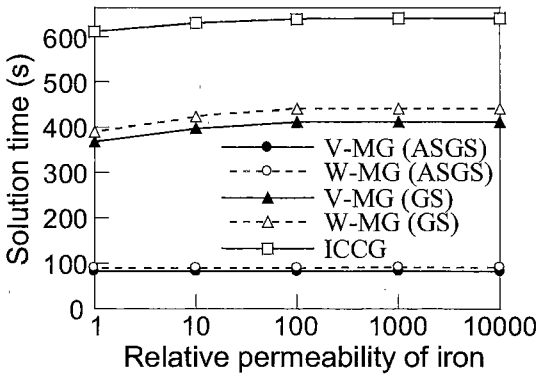

Fig. 5. Effect of iron permeability on the solution time.

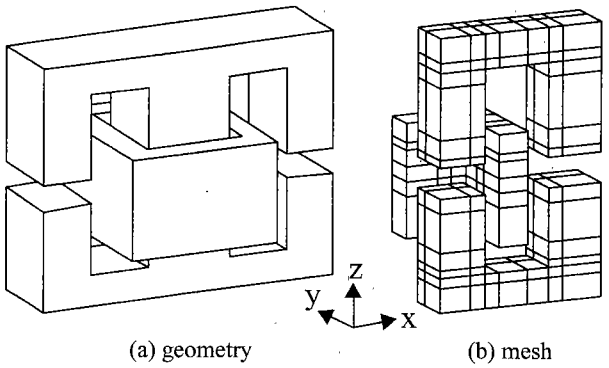

Fig. 6. Geometry and mesh of one fourth of the electromagnet.

the increase of the aspect ratio, n_{si} needs also to be increased. At $R_{\max} = 30$ MGM with ASGS is the fastest with $n_{si} = 13$, while MGM with GS is the fastest with $n_{si} = 15$. At $R_{\max} = 100$ MGM with ASGS is the fastest with $n_{si} = 20$.

In order to test the robustness of MGM with ASGS against parameter variations, the relative permeability of the iron core of the model in Fig. 3(a) is varied from 1 till 10000. The mesh with maximum element aspect ratio $R_{\max} = 15$ shown in Fig. 3(b) is analyzed. Meshes with such aspect ratio are common for the practical MGM. The solution times for the different relative permeabilities of iron for this mesh are given in Fig. 5.

Fig. 5 shows that both MGM with GS and FEM with ICCG are sensitive to the parameter variations, because their solution times increase with the increase of the relative permeability of iron. In contrast, the proposed MGM with ASGS is robust against parameter variations, since the computation time does not depend on the iron core permeability.

The second example is an E-type ac electromagnet shown in Fig. 6(a). The number of turns and resistance of the exciting coil are 2700 and 232 Ω, respectively. The exciting current is 0.64 A and the air gap is 6 mm. The relative permeability of iron is 1000.

Having almost 2 million unknowns at the finest level, this example allows to validate and to analyze the performance of MGM with ASGS for large-scale problems.

Due to the symmetry, one quarter of the electromagnet is analyzed. The FEM formulation is given by (1).

Table 2. Discretization data for the electromagnet.

Level	No. of unknowns	No. of elements
1	4567	1260
2	33318	10080
3	254092	80640
4	1983768	645120

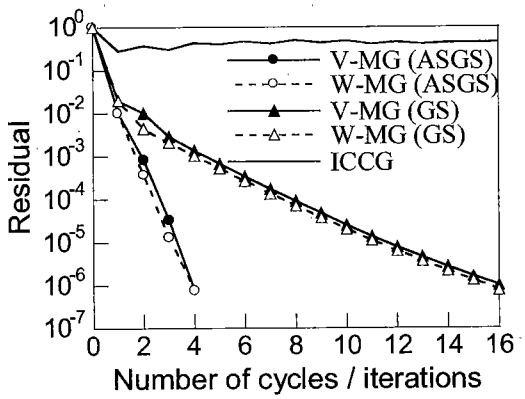

Fig. 7. Number of iterations for the electromagnet.

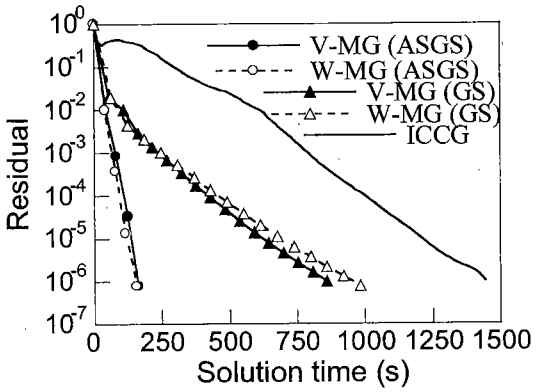

Fig. 8. Convergence rate for the electromagnet.

Edge hexahedra are used. The finite element mesh is shown in Fig. 6(b). The maximum element aspect ratio for this example is $R_{\max} = 15$.

The numerical analysis is carried out by the V-cycle, W-cycle and the full MGM with four nested meshes detailed in Table 2.

The convergence behavior of the V-cycle and W-cycle MGM applied to the electromagnet is shown in Fig. 7. The results from Fig. 7 indicate that MGM with ASGS needs the smallest number of cycles. There is no difference in the number of cycles for the V- and W- cycle MGM. The scaled ICCG method is the slowest with 520 iterations.

The solution times of the V-cycle and W-cycle MGM are shown in Fig. 8. As seen in Fig. 8, MGM with ASGS is the fastest among the methods. The V-cycle and W-cycle MGM with ASGS result in close solution times.

For this model, MGM with ASGS is the fastest with $n_{si} = 8$, while MGM with GS is the fastest with $n_{si} = 17$.

Although the V-cycle and the W-cycle multigrid algorithms are usually very efficient, the speed of MGM in some cases can still be improved using nested iteration,

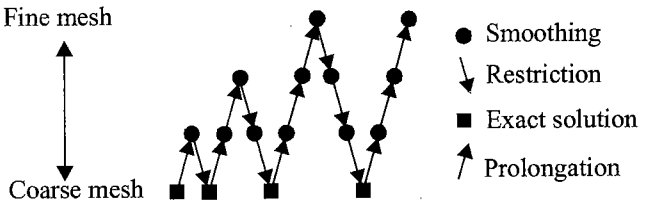

Fig. 9. V-cycle full multigrid algorithm with four levels.

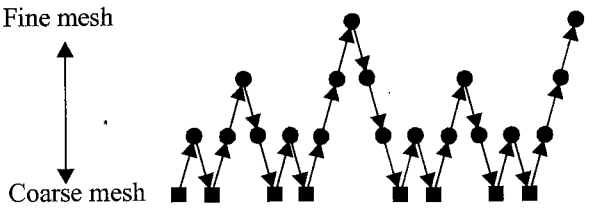

Fig. 10. W-cycle full multigrid algorithm with four levels.

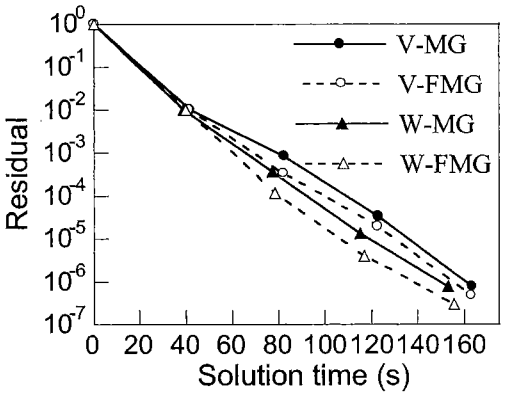

Fig. 11. Solution times for the V-cycle, W-cycle and full multigrid using ASGS.

also called full multigrid (FMG) [1] [10]. In FMG the solution on the coarse mesh is used as initial guess for the approximation on the finer grid. The algorithms of the V-cycle FMG (V-FMG) and the W-cycle FMG (W-FMG) are shown in Fig. 9 and in Fig. 10, respectively.

Fig. 11 compares the solution times of the V-cycle, W-cycle and full multigrid applied to the electromagnet. Only MGM with ASGS is analyzed due to its superiority to MGM with GS.

The results from Fig. 11 indicate that the V-cycle MGM and the full V-cycle MGM yield almost the same solution times that are 133.38 s and 133.22 s, respectively. Hence in case of the V-cycle there is no significant gain from the full multigrid method.

The solution times for the W-cycle MGM and the full W-cycle MGM are 153.03 s and 155.63 s, respectively. Therefore the W-cycle MGM is preferable to the full W-cycle MGM.

Next we shall try to speed-up the performance of the edge MGM by changing the values of the parameter c in (5). Details about the proper choice of c in the case of nodal finite elements can be found in reference (11).

Fig. 12 shows the influence of the parameter c on the solution times by the V-cycle, W-cycle and full multigrid with ASGS applied to the electromagnet.

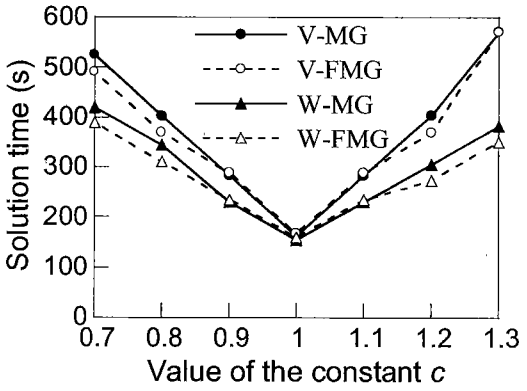

Fig. 12. Solution times vs. the parameter c for the V-cycle, W-cycle and full multigrid using ASGS.

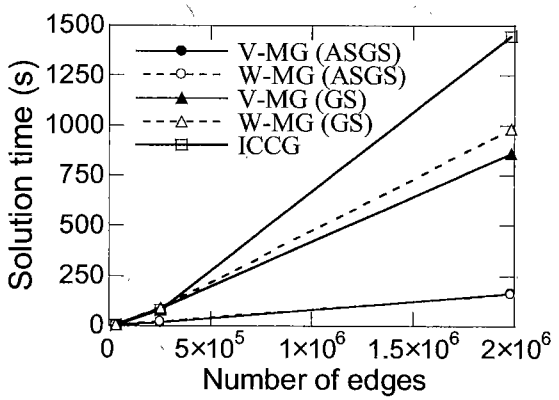

Fig. 13. Solution time versus number of unknowns.

The results from Fig. 12 clearly indicate that the V-cycle, W-cycle and full multigrid using ASGS are the fastest for the value of parameter $c = 1$.

The most time consuming part of the multigrid cycle is the solution of the set of equations at the finest mesh. Therefore in the next section the solution times of the MGM with ASGS will be compared to MGM with GS and the FEM with scaled ICCG for different number of multigrid (MG) levels. As shown in Fig. 11, there is no significant gain from the full multigrid method. For this reason only the V-cycle and W-cycle MGM will be analyzed.

Fig. 13 compares the solution times of the different methods applied to the electromagnet when the number of multigrid levels is changed from 2 to 4.

Fig. 13 shows that when the accelerated symmetric Gauss-Seidel smoother is used, the V- and W-cycle MGM have stable and fast convergence rate and result in similar solution times. When the Gauss-Seidel smoother is used, however, the W-cycle MGM is slower than the V-cycle and the difference in solution times increases with the number of unknowns. This is due to the fact that MGM with GS needs more cycles than MGM with ASGS and the number of computer operations per one W-cycle is greater than that of the V-cycle, as seen in Fig. 1.

Fig. 13 indicates that MGM with ASGS is faster than the other methods even for only two MG levels with 33318 unknowns. With two levels the V-cycle MGM with ASGS needs only 4 cycles (2.41 s) to reduce the residual by a factor of 10^{-6}. The V-cycle MGM with GS and ICCG need 13 cycles (8.09 s) and 125 iterations (5.07 s), respectively.

Table 3. Discretization data for the electromagnet.

No. of unknowns	Computed force (N)		
	MGM with ASGS	MGM with GS	FEM with ICCG
33318	18.24	18.24	18.24
254092	18.64	18.64	18.64
1983768	18.93	18.93	18.93
Measured force: 20.1 (N)			

When four levels with 1983768 unknowns are used, MGM with ASGS is about five times faster than MGM with GS and nine times faster than FEM with the ICCG method. It takes only 4 cycles (163.42 s) for the V-cycle MGM with ASGS to reduce the residual by a factor of 10^{-6}. The V-cycle MGM with GS and the ICCG method need 16 cycles (859.59 s) and 520 iterations (1446.33 s), respectively. Therefore it can be concluded that the efficiency of MGM with ASGS increases strongly with the number of unknowns on the finest level.

Fig. 13 indicates that the solution time of MGM with ASGS increases only linearly with the number of unknowns. This shows that MGM with ASGS has optimal complexity.

5. Validation of MGM with ASGS

In order to validate the proposed MGM with ASGS, the electromagnetic force acting on the movable armature of the electromagnet in Fig. 6 is computed and compared with measurements. The force $\boldsymbol{F}$ is obtained by the Maxwell stress tensor method:

$$\boldsymbol{F} = \int_S \nu_0 \left[(\boldsymbol{Bn})\boldsymbol{B} - 0.5\boldsymbol{B}^2\boldsymbol{n} \right] d\Omega \quad \cdots\cdots\cdots (6)$$

S in (7) is a closed surface surrounding the moving object, ν_0 is the reluctivity of air, $\boldsymbol{B}$ is the magnetic flux density and $\boldsymbol{n}$ is an outward unit vector normal to the surface S. In our analysis S passes through the middle of the air gap.

Thus the force F_e^z of one finite element acting along the z axis is:

$$F_e^z = \nu_0 [(n_e^x B_e^x + n_e^y B_e^y + n_e^z B_e^z) B_e^z - 0.5 B_e^2 n_e^z] S_e \quad \cdots\cdots\cdots\cdots (7)$$

S_e in (8) is the area obtained when intersecting the element with the integration surface. The superscripts x, y and z designate the components along the three axes. The total force is equal to the sum of the forces of all intersected elements.

Table 3 shows the force computed by MGM with ASGS, MGM with GS, FEM with ICCG and the measured force. The computed values of force by the V-cycle, W-cycle and the full MGM were similar. Therefore only one computed result is given for the different MG algorithms in Table 3.

There is a good agreement between the computed and

measured force in Table 3, which confirms the validity of the proposed MGM with ASGS.

6. Conclusions

A fast edge element geometric multigrid method with accelerated symmetric Gauss-Seidel smoother is presented. The convergence and speed of the V-cycle, W-cycle and full multigrid method using this smoother are analyzed. The performance of MGM using ASGS is compared with that of MGM with Gauss-Seidel and the FEM with scaled ICCG method. Unlike MGM with the conventional Gauss-Seidel, the multigrid method with the newly proposed accelerated symmetric Gauss-Seidel smoother is robust against mesh distortion and parameter variations. MGM with ASGS is much faster and needs less cycles than MGM with GS and FEM with the ICCG method not only for large-size problems, but also for problems with small number of unknowns and levels. The validity of the MGM with accelerated symmetric Gauss-Seidel smoother is confirmed by comparing the computed and measured force of an electromagnet.

Acknowledgment

This work was supported by the Japan Society for the Promotion of Science (JSPS) under Grant-in-Aid for Scientific Research No.12000743-00.

(Manuscript received July 8, 2002,
revised April 28, 2003)

References

(1) V. Cingoski, R. Tokuda, S. Noguchi, and H. Yamashita: "Fast multigrid solution method for nested edge-based finite element meshes", *IEEE Trans. Magn.*, Vol.36, No.4, pp.1539–1542 (2000-7)

(2) A. Kameari: "Application of geometrical multigrid method to electromagnetic computation by finite element method", *The Papers of Joint Technical Meeting on Static Apparatus and Rotating Machinery, IEE Japan*, SA-01-11, RM-01-79, pp.61–66 (2001-8) (in Japanese)

(3) B. Weiss and O. Biro: "Edge element multigrid solution of nonlinear magnetostatic problems", *Compel*, Vol.20, No.2, pp.357–365 (2001)

(4) M. Schinnerl, J. Shoberl, and M. Kaltenbacher: "Nested multigrid methods for the fast numerical computation of 3D magnetic fields", *IEEE Trans. Magn.*, Vol.36, No.4, pp.1557–1560 (2000-7)

(5) K. Kondo, K. Watanabe, H. Igarashi, and T. Honma: "On mesh dependence of multigrid method for finite element analysis of three-dimensional magnetostatic fields", *Proc. of 14th Symposium on Electromagnetics and Dynamics (SEAD)*, pp.93–96 (2002-5) (in Japanese)

(6) V. Spasov, S. Noguchi, and H. Yamashita: "Fast finite element analysis by 3D geometric multigrid with edge elements", *Proc. of 11th Magnetodymanics (MAGDA) Conference*, pp.246–249 (2002-3)

(7) J. Jin: *The finite element method in electromagnetics*, John Wiley & Sons, Inc., New York (1993)

(8) A. Kameari and K. Koganezawa: "Convergence of ICCG method in FEM using edge elements without gauge condition", *IEEE Trans. Magn.*, Vol.33, No.2, pp.1223–1226 (1997-3)

(9) K. Fujiwara, T. Nakata, N. Takahashi, and H. Ohashi: "On the continuity of the magnetizing current density in 3-D magnetic field analysis with edge element", *IEEE Trans. Magn.*, Vol.31, No.3, pp.1364–1367 (1995-5)

(10) P. Wesseling: An introduction to multigrid methods, p.70, John Wiley & Sons, Inc., New York (1992)

(11) K. Tsubota, S. Noguchi, and H. Yamashita: "Speed-up for finite element analysis by using multigrid method", *IEEJ Trans. IA*, Vol.121, No.10, pp.1017–1023 (2001-10) (in Japanese)

(12) F.L. Hageman: Applied iterative methods, Academic Press (1981)

(13) G. Golub, et al.: Matrix computations, 3rd ed., pp.516–517, The Johns Hopkins University Press (1996)

(14) W. Hackbush: Multi-grid methods and applications, Springer-Verlag (1985)

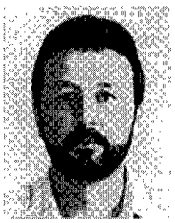

Vasil Spasov (Non-member) received his Ph.D. degree from the Technical University in Sofia, Bulgaria in 1999. He has been assistant professor at the Technical University in Plovdiv, Bulgaria since 1993. He specialized at the Nottingham Trent University, Nottingham, UK in 1995. From July 2000 till July 2002 he was a Postdoctoral Research Fellow at the Graduate School of Engineering, Hiroshima University. The fellowship was awarded by the Japan Society for the Promotion of Science (JSPS). His research interests are in the area of the electromagnetic field analysis by the Multigrid Method and the Finite Element Method. He is a member of the International Compumag Society (ICS).

So Noguchi (Member) received his Dr.Eng. from Waseda University in 1999. He is a research associate in Graduate School of Engineering at Hiroshima University since 1999. His research interests are applied superconductivity, numerical analysis in electromagnetics and optimal design method. He is a member of the IEEE, the IEE of Japan, and the Japan Society of Applied Electromagnetics.

Hideo Yamashita (Member) received the B.E. and M.E. degrees in electrical engineering from Hiroshima University, Hiroshima, Japan, in 1964 and 1968, and Dr. of Engineering degree in 1977 from Waseda University, Tokyo, Japan. Since 1992 he has been a Professor at Faculty of Engineering, Hiroshima University. He was an Associate Researcher at Clarkson University, Potsdam, N.Y. in 1981–1982. His research interests lie in the area of scientific visualization, computer graphics and the magnetic field analysis by Numerical Methods. He is a member of the IEEE, the IEE of Japan, the IECE of Japan, the IPS of Japan, the Japan Society for Simulation Technology, and the Japan Society of Applied Electromagnetics.